Wavelike statistics from pilot-wave dynamics in a circular corral

Daniel M. Harris,[1,*] Julien Moukhtar,[2] Emmanuel Fort,[3] Yves Couder,[2] and John W. M. Bush[1,†]

[1]*Department of Mathematics, Massachusetts Institute of Technology, Cambridge, Massachusetts 02139, USA*

[2]*Laboratoire Matières et Systèmes Complexes, Université Paris Diderot and CNRS-UMR 7057, Bâtiment Condorcet, 10 rue Alice Domon et Léonie Duquet, 75013 Paris, France*

[3]*Institut Langevin, ESPCI ParisTech, Université Paris Diderot and CNRS-UMR 7587, 10 rue Vauquelin, 75231 Paris Cedex 05, France*

Bouncing droplets can self-propel laterally along the surface of a vibrated fluid bath by virtue of a resonant interaction with their own wave field. The resulting walking droplets exhibit features reminiscent of microscopic quantum particles. Here we present the results of an experimental investigation of droplets walking in a circular corral. We demonstrate that a coherent wavelike statistical behavior emerges from the complex underlying dynamics and that the probability distribution is prescribed by the Faraday wave mode of the corral. The statistical behavior of the walking droplets is demonstrated to be analogous to that of electrons in quantum corrals.

PACS number(s): 47.55.D−, 47.85.−g, 03.65.−w

When a horizontal fluid bath is vibrated vertically in a sinusoidal fashion with peak acceleration γg (g being the gravitational acceleration) and frequency f, there is a critical acceleration $\gamma_F g$ above which its free surface becomes unstable to standing Faraday waves with frequency $f/2$ [1,2]. Below this Faraday threshold, when the interface would otherwise remain flat, a millimetric droplet may be levitated on the vibrating bath surface [3]. Provided the air layer between the droplet and bath is sustained during impact, coalescence is precluded and the drop may bounce indefinitely [4,5]. When the bouncing is of sufficient amplitude to have twice the forcing period, the droplet achieves resonance with its Faraday wave field, as is generated by its impacts. When this resonance is achieved and the forcing acceleration exceeds the walking threshold $\gamma > \gamma_w$, the bouncing drop is destabilized by its wave field, giving way to a stable walking state marked by steady horizontal motion [6,7]. Millimetric droplets can thus walk on a vibrating fluid bath through a resonant interaction with their own wave field. The resulting physical picture, in which the droplet is piloted by a guiding wave field, is reminiscent of that proposed by de Broglie as the basis of a rational quantum mechanics, pilot-wave dynamics [8].

The propulsive wave force originates from the droplet landing on a sloping surface. The local slope is determined by the wave field generated by previous impacts and so depends on both the droplet's path and the spatiotemporal extent of its wave field. The dynamics of the walking droplets, henceforth walkers, is thus non-Markovian: Predicting the evolution of the system requires knowledge not only of its present state, but of its past. The concept of path memory was thus introduced to characterize the influence of the walker's past on the propulsive wave force [9], a concept that is quantified in the theoretical developments of Moláček and Bush [7]. As the forcing acceleration is increased progressively from the walking threshold $\gamma_w g$ towards the Faraday threshold $\gamma_F g$, the amplitude of the waves increases, their decay rate decreases, and the path memory increases progressively. In an unbounded geometry, the walkers propel themselves in a straight line at a uniform speed that typically increases with increasing memory. In more complex geometries, the interaction of the guiding wave field with boundaries leads to relatively rich dynamics and complex trajectories [10,11]. In the long-path-memory limit, the walking droplets exhibit several features previously thought to be exclusive to the microscopic quantum realm, including single-particle diffraction, tunneling, quantized orbits, and orbital level splitting [4,6,10–14].

Couder and Fort [10] demonstrated the diffraction of individual walkers as they passed through both single- and double-slit geometries, in response to the diffraction of their guiding waves. As a single walker passes through a slit, it appears to be randomly deflected; however, in the long-path-memory limit, repetition of the experiment reveals the emergence of a coherent wavelike statistical behavior. Specifically, the probability of a particular deflection angle is prescribed by the relative far-field amplitude of a linear plane wave with the Faraday wavelength impinging on the slits. Thus, as in quantum mechanics, the statistical behavior of the system can be described by a wave function that satisfies a linear wave equation.

We here examine the dynamics and statistics of droplets walking in a confined circular geometry [see Fig. 1(a)] [15]. The bath consists of a relatively deep layer surrounded by a shallow layer, the depths chosen to ensure that the droplet can only walk in the deep corral region. The walker is thus confined to the corral, while its guiding wave field is influenced by reflections off the corral edges. Figure 1(b) illustrates the cavity mode just above the Faraday threshold at the driving frequency considered. For our walker experiments, the forcing amplitude is always below the Faraday threshold, so the free surface would remain flat in the absence of the droplet. We follow the walker's trajectory with particle-tracking software. We proceed by describing the dependence of the walker dynamics on the proximity to the Faraday threshold, which can be characterized by the dimensionless parameter $\Gamma = (\gamma_F - \gamma)/\gamma_F$. As Γ approaches zero, the path memory necessarily increases.

————————
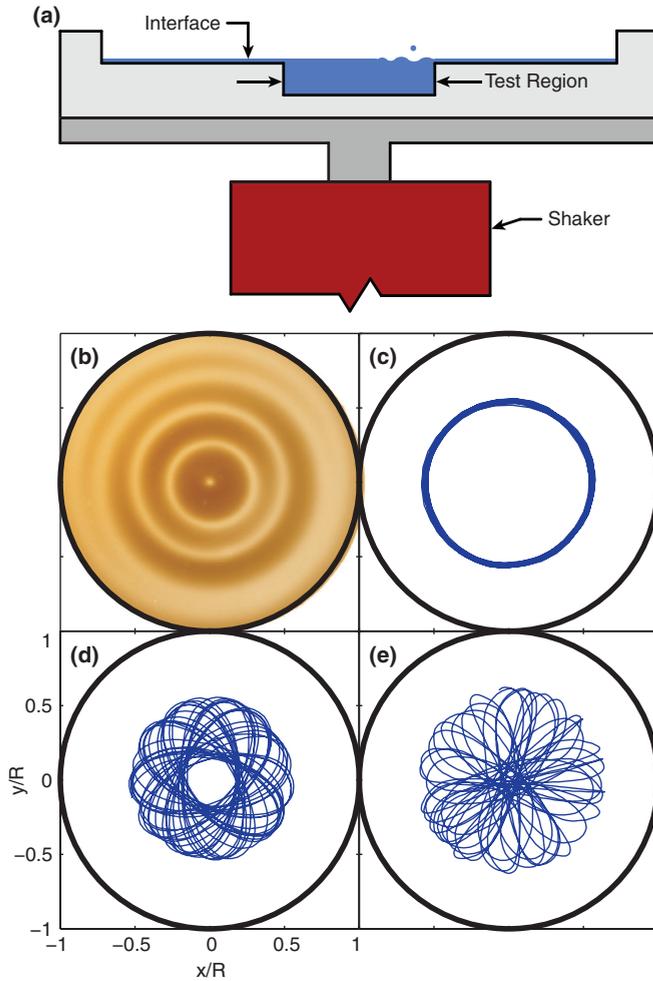*dmh@math.mit.edu

†Corresponding author: bush@math.mit.edu

FIG. 1. (Color online) (a) Schematic illustration of the experimental apparatus, a fluid bath driven vertically in a sinusoidal manner with amplitude A_0 and frequency f. (b) Faraday mode in a circular corral of radius $R = 10.1$ mm and depth $h_0 = 5$ mm, driven at $f = 80$ Hz, for which $\gamma_F = 4.6$ and the Faraday wavelength is $\lambda_F = 4.75$ mm. The frequency was selected to ensure that the wave field just above the Faraday threshold was stationary. Note that the bright rings correspond to areas of small surface slope, indicating local extrema of wave amplitude. (c)–(e) Typical trajectories of a walker with diameter $D = 0.8$ mm with mean velocity $\bar{v} = 11$ mm/s in the same circular corral at (c) low memory $\Gamma = 0.18$ and intermediate memories (d) $\Gamma = 0.1$ and (e) $\Gamma = 0.06$.

Figure 1(c) illustrates the circular trajectory of a walker with short path memory in a circular cavity. As the path memory is increased progressively, this circular orbit becomes unstable, giving way to a epicycloidal trajectories with increasing deviations from the unstable circle [Figs. 1(d) and 1(e)] [15]. Figure 2 illustrates sample images of a walker and its guiding wave field in the long-path-memory limit. The walker's pilot-wave field is continuously evolving: While its peak amplitude is generally near the point of the droplet's last impact, its detailed form depends on the droplet's past trajectory. At any instant, the wave field is complex, the result of a superposition of waves created by the droplet's previous bounces: In general, it bears no resemblance to the resonant wave mode of the cavity. The dynamics in the long-path-memory limit thus
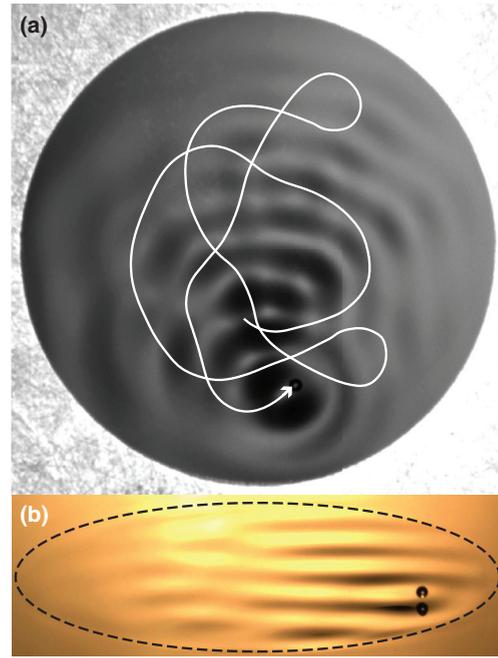

FIG. 2. (Color online) (a) Top view of a walker exploring a circular corral in the long-path-memory limit. Its complex pilot-wave field is apparent; its trajectory is indicated in white. (b) Oblique view of a walker and its pilot wave exploring a circular corral. The dashed line indicates the edge of the corral.

cannot be simply rationalized in terms of stochastic motion modulated by the wave mode of the cavity. On the contrary, this pilot-wave dynamics has certain distinct features. Specifically, the monochromatic guiding wave field constrains the radius of curvature, which rarely takes values less than half the Faraday wavelength. The complex guiding wave field in this long-memory limit thus renders the walker's trajectory relatively smooth, but its dynamics chaotic. We note that this smooth pilot-wave dynamics is markedly different from that observed when the system is driven above the Faraday threshold, when the trajectory is relatively erratic and marked by sharp changes in direction.

Figure 3(a) illustrates sample trajectories of increasing length, which have been color coded according to the droplet speed. We note that in the absence of boundaries, the walker speed would remain constant and its motion rectilinear. In this long-memory limit, the walker's trajectory is complex, owing to the interaction of its extended pilot-wave field with the boundaries; moreover, the walker speed varies significantly from its mean ($\bar{v} = 8.66$ mm/s) along its path. In the long-time limit, a pattern emerges in the velocity fluctuations, a pattern that is echoed in the droplet statistics. The probability distribution presented in Fig. 3(b) indicates the emergence of a coherent wavelike statistical behavior for the walking droplet.

The axially symmetrized histogram is shown in Fig. 4(a) along with the amplitude of the cavity mode $|J_0(k_F r)|$ with the Faraday wavelength $\lambda_F = 2\pi/k_F$, as predicted by linear theory [2]. The correspondence between the two indicates that, as in quantum mechanics, the statistics of a confined particle can be prescribed by a wave function satisfying a linear wave equation. If one fits the data to a linear superposition of cavity
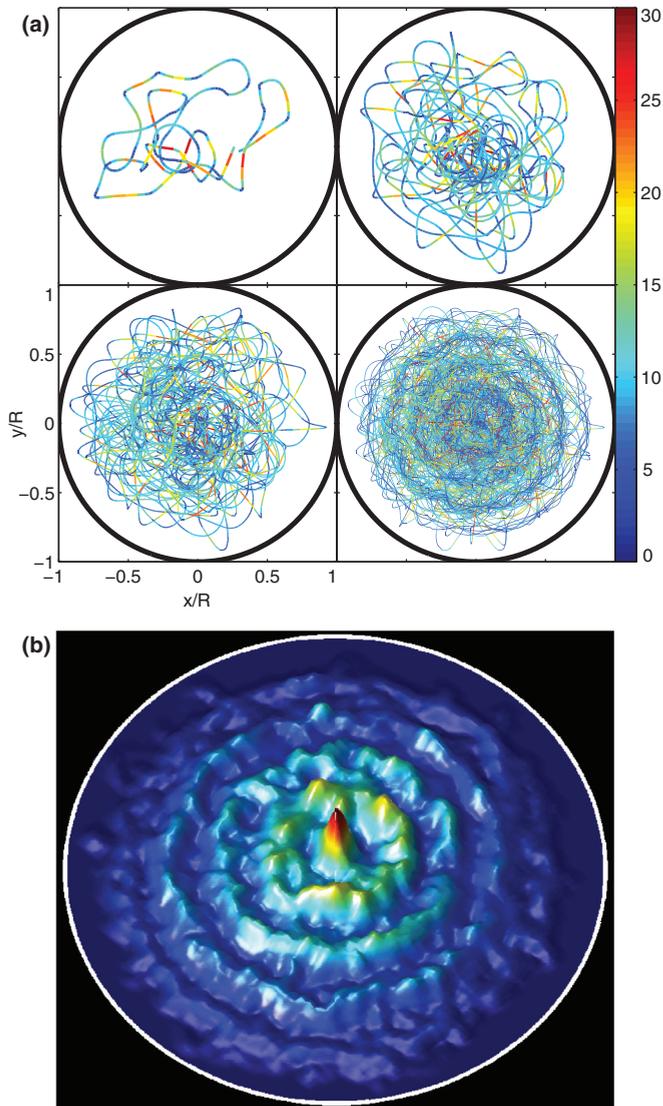
FIG. 3. (Color) (a) Trajectories of a droplet of diameter $D = 0.67$ mm walking in a circular corral with radius $R = 14.3$ mm and depth $h_0 = 6.6$ mm, driven at $f = 70$ Hz, for which $\gamma_F = 3.7$. Trajectories of increasing length in the long-path-memory limit ($\Gamma = 0.011$) are color coded according to droplet speed (mm/s). (b) Probability distribution of the walking droplet's position.
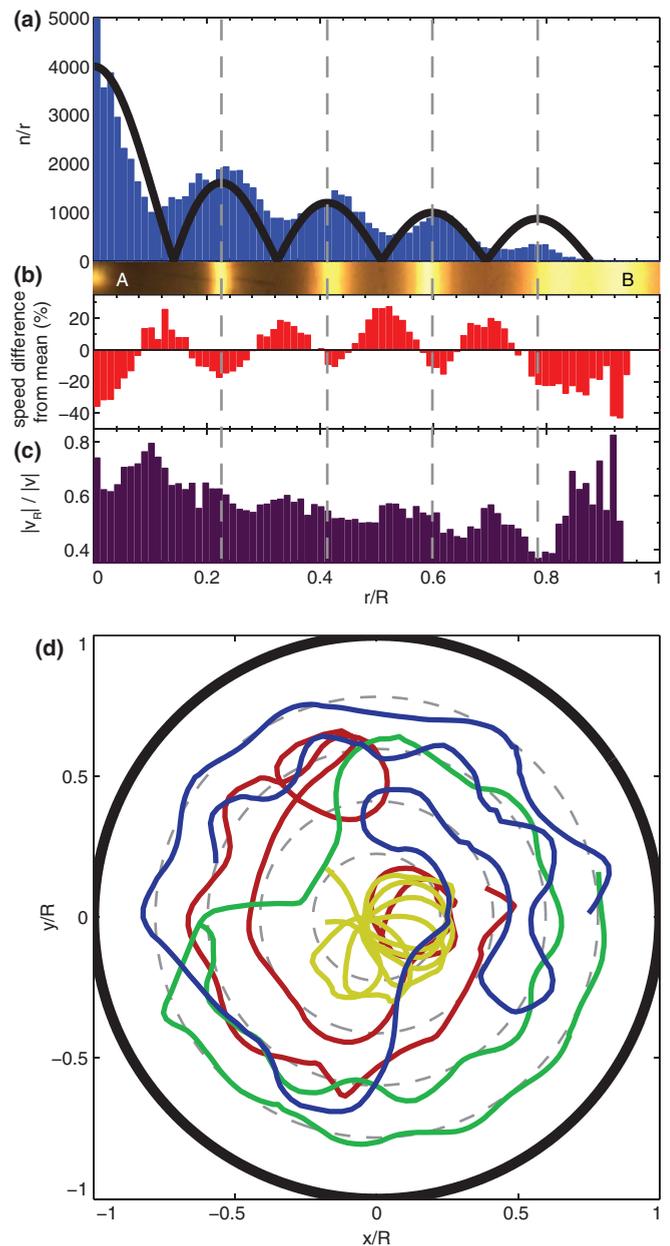

FIG. 4. (Color) (a) Histogram of radial position, (b) velocity variation from the mean ($|\bar{v}| = 8.66$ mm/s), and (c) radial dependence of the normalized radial velocity ($|v_R|/|v|$). In (a), the minima in the probability amplitude approximately correspond to maxima in the walker velocity, maxima in the normalized radial velocity, and zeros in the amplitude of the fundamental cavity mode (upper curve). The section A-B represents a radial slice of the cavity's Faraday mode, with bright bands indicating local extrema. Averaging windows and bin widths are fixed at $0.012R$. In (c), values of 1 and 0 correspond to purely radial and azimuthal motion, respectively. (d) Four sample trajectories extracted from the complete trajectory indicate a tendency to orbital motion along particular radii. Different colors serve only to demarcate different trajectories. In all plots, the dashed lines represent maxima in the amplitude of the fundamental cavity mode.

eigenmodes with wavelength closest to λ_F, the fit can be slightly improved and the zeros in the predicted probability amplitude disappear. However, this requires the introduction of additional fitting parameters, namely, the amplitude ratio of each mode, so for simplicity we compare only to a single mode. Doing so indicates that the walker's probability distribution is well approximated by the amplitude of the linear Faraday wave mode of the corral.

There are several features of this pilot-wave dynamics that contribute to the emergence of the coherent wavelike statistical pattern. In Fig. 4(b) we demonstrate that fluctuations in the walker's speed are correlated with its radial position, as was suggested by the color-coded trajectories presented in Fig. 3(a). In general, the walker's speed is lowest at the locations of maximum amplitude of the fundamental cavity

mode, augmenting the probability amplitude at these radii. The spatial distribution of the normalized radial velocity is presented in Fig. 4(c), where we again observe a spatial

periodicity, with the locations of the peaks corresponding roughly to the zeros in the amplitude of the cavity mode. This correlation may be rationalized in terms of the walkers' tendency to move azimuthally about preferred radii and radially in between, as is exemplified in sample trajectories reported in Fig. 4(d). We can thus understand the probability distribution as being a manifestation of the characteristics of the underlying trajectories. In the confined circular geometry, the pilot-wave dynamics tends to drive the walker along circular orbits with radii corresponding to maxima of the cavity mode amplitude. Instead of being trapped on these orbits as in the low-path-memory limit [Fig. 1(c)], the walker wobbles around them and drifts between them; nevertheless, these unstable orbits leave their mark on the probability distribution.

We have examined the hydrodynamic analog of a quantum particle in a circular domain, demonstrating the emergence of a coherent statistical behavior in the long-memory limit. Our results indicate that the statistical behavior is rooted in the wave-induced spatial dependence of the walking speed and the tendency for the walker to trace out the unstable orbital states of the cavity. The experiments reported herein indicate that in the long-memory limit, walkers in confined geometries, like quantum particles, have a coherent statistical behavior that may be characterized by a linear wave theory. Whether or not the statistical description provided by quantum mechanics represents a complete description of physical reality was the subject of the celebrated debate between Einstein [16] and Bohr [17]. Whatever the case may be in quantum mechanics, the linear statistics is clearly an incomplete description of our fluid system and is underlaid by a complex, nonlinear, pilot-wave dynamics.

It is interesting to consider our results in light of quantum corral experiments, in which electrons are confined to a corral composed of iron adatoms on the surface of a copper substrate [18–20]. We note that the spacing between the adatoms results in considerable energy loss, as do the shallows surrounding our fluid corrals. The electron density in the quantum corral was measured with a scanning-electron microscope and found to have a wavelike pattern with the de Broglie wavelength of the trapped electrons λ_{dB}. The probability distribution presented in Fig. 3(b) is thus analogous to that in the circular quantum corral, with λ_F playing the role of λ_{dB}.

In our fluid system, we are able to observe not only an analogous statistical wave [Fig. 3(b)], but a real physical wave that guides the droplet (Fig. 2). While in unbounded geometries the pilot-wave field assumes a relatively simple form [9] and gives rise to rectilinear motion, in the corral geometry, its form is affected by reflections off the boundaries and the resulting walker motion is irregular, with the degree of irregularity increasing with path memory. As was the case in the study of single-particle diffraction [10], in the long-path-memory limit, the statistical wave function is prescribed by the wavelength of the pilot wave and the system geometry. We note that similar results arise for a walker confined to walk along a line in a narrow rectangular geometry, where the wavelength of the probability distribution is again prescribed by that of the guiding wave. A discussion of the results obtained in this geometry is beyond the scope of the present paper.

Our study indicates that this hydrodynamic system is closely related to the physical picture of quantum dynamics envisaged by de Broglie, in which rapid oscillations originating in the particle give rise to a guiding wave field [8,21,22]. The pilot-wave theories of de Broglie and Bohm [23] are often conflated [24]; however, it is valuable to distinguish between them here for the sake of comparison with our system. According to Bohm, the particle is guided by its statistical wave, its velocity being equivalent to the quantum velocity of probability. According to de Broglie's double-wave solution [8], the particle is guided by a real wave (of unspecified origins) in such a way as to execute a dynamics whose statistics is described by standard quantum theory. Figure 2(a) indicates the instantaneous surface wave field responsible for piloting the walker, whose complex form results in a complex trajectory. Figure 3(b) represents the relatively simple statistical wave field describing the probability distribution, whose form is prescribed by the eigenmode of the cavity. The simple form of the statistical wave conceals the complex underlying pilot-wave dynamics.

[1] M. Faraday, Philos. Trans. R. Soc. London **121**, 319 (1831).

[2] T. B. Benjamin and F. Ursell, Proc. R. Soc. London Ser. A **225**, 505 (1954).

[3] J. Walker, Sci. Am. **238** (6), 151 (1978).

[4] Y. Couder, E. Fort, C.-H. Gautier, and A. Boudaoud, Phys. Rev. Lett. **94**, 177801 (2005).

[5] J. Moláček and J. W. M. Bush, J. Fluid Mechanics **727**, 582 (2013).

[6] S. Protière, A. Boudaoud, and Y. Couder, J. Fluid Mech. **554**, 85 (2006).

[7] J. Moláček and J. W. M. Bush, J. Fluid Mechanics **727**, 612 (2013).

[8] L. de Broglie, *Ondes et Mouvements* (Gautier Villars, Paris, 1926).

[9] A. Eddi, E. Sultan, J. Moukhtar, E. Fort, M. Rossi, and Y. Couder, J. Fluid Mech. **674**, 433 (2011).

[10] Y. Couder and E. Fort, Phys. Rev. Lett. **97**, 154101 (2006).

[11] A. Eddi, E. Fort, F. Moisy, and Y. Couder, Phys. Rev. Lett. **102**, 240401 (2009).

[12] E. Fort, A. Eddi, A. Boudaoud, J. Moukhtar, and Y. Couder, Proc. Natl. Acad. Sci. **107**, 17515 (2010).

[13] J. W. M. Bush, Proc. Natl. Acad. Sci. **107**, 17455 (2010).

[14] A. Eddi, J. Moukhtar, S. Perrard, E. Fort, and Y. Couder, Phys. Rev. Lett. **108**, 264503 (2012).

[15] See Supplemental Material at http://link.aps.org/supplemental/10.1103/PhysRevE.88.011001 for complete experimental methods and movies of a walking droplet confined to a circular geometry.

[16] A. Einstein, B. Podolsky, and N. Rosen, Phys. Rev. **47**, 777 (1935).

[17] N. Bohr, Phys. Rev. **48**, 696 (1935).

[18] M. F. Crommie, C. P. Lutz, and D. M. Eigler, Nature (London) **363**, 524 (1993).

[19] M. F. Crommie, C. P. Lutz, and D. M. Eigler, Science **262**, 218 (1993).

[20] G. A. Fiete and E. J. Heller, Rev. Mod. Phys. **75**, 933 (2003).

[21] L. de Broglie, Ann. Fond. Louis de Broglie **12**, 1 (1987).

[22] Y. Couder and E. Fort, J. Phys.: Conf. Ser. **361**, 012001 (2012).

[23] D. Bohm, Phys. Rev. **85**, 166 (1952).

[24] P. Holland, *The Quantum Theory of Motion: An Account of the de Broglie–Bohm Causal Interpretation of Quantum Mechanics* (Cambridge University Press, Cambridge, 1993).